

Continuum Theory of Polymer Crystallization

Arindam Kundagrami and M. Muthukumar^{a)}

*Department of Polymer Science and Engineering
University of Massachusetts at Amherst, Amherst, MA 01003*

We present a kinetic model of crystal growth of polymers of finite molecular weight. Experiments help to classify polymer crystallization broadly into two kinetic regimes. One is observed in melts or in high molar mass polymer solutions and is dominated by nucleation control with $G \sim \exp(1/T\Delta T)$, where G is the growth rate and ΔT is the super-cooling. The other is observed in low molar mass solutions (as well as for small molecules) and is diffusion controlled with $G \sim \Delta T$, for small ΔT . Our model unifies these two regimes in a single formalism. The model accounts for the accumulation of polymer chains near the growth front and invokes an entropic barrier theory to recover both limits of nucleation and diffusion control. The basic theory applies to both melts and solutions, and we numerically calculate the growth details of a single crystal in a dilute solution. The effects of molecular weight and concentration are also determined considering conventional polymer dynamics. Our theory shows that entropic considerations, in addition to the traditional energetic arguments, can capture general trends of a vast range of phenomenology. Unifying ideas on crystallization from small molecules and from flexible polymer chains emerge from our theory.

a)Author to whom correspondence should be addressed. E-mail: muthu@polysci.umass.edu

I. INTRODUCTION

There are several different processes involved in crystal growth from molecules of both low and high molecular weight; they become more complex for flexible macromolecules or polymers. Extensive experiments on the growth kinetics of lamellae in solutions and melts helped to classify the growth rates broadly into two universality classes. In the first, valid

for melt-grown crystals and solution-grown crystals of relatively high molecular weight, the growth rate G depends exponentially on the variable $1/T_c\Delta T^{1,2,3,4}$ as,

$$G \sim \exp \left[\frac{-\mathcal{P}}{T_c\Delta T} \right], \quad (1.1)$$

where, $\Delta T = T_m - T_c$ is the super-cooling with T_m and T_c , respectively, as the crystallization temperature and the equilibrium melting temperature, and \mathcal{P} is a parameter. In the second class, valid for solution-grown crystals of relatively low molecular weight, the growth rate goes linearly with super-cooling as,

$$G \sim \Delta T, \quad (1.2)$$

for small ΔT . In this paper, we have developed a model that unifies these two apparently different physical processes and allows us to capture the limiting behaviours of both classes.

In a highly complex growth phenomenon such as polymer crystallization involving a multitude of processes, the rate determining factor is the one which impedes the growth more than any other. For example, the entanglement effect of interpenetrating polymer chains must be crucial to the kinetics in melt-grown crystals or solution-grown crystals of high molar mass, whereas free diffusion or transport effects are possibly dominant in solution-grown crystals of low molar mass. The generic growth rates in polymer crystallization (10^{-3} to $10\mu\text{m/hr.}$)^{2,3,4} are orders of magnitude lower than that expected in a diffusion-limited crystal growth (10 to $10^5\mu\text{m/hr.}$)^{5,6,7,8,9}. This immediately suggests the presence of some sort of a barrier or 'entropic tension' at or near the growth front of a polymer crystal. In quantitative terms, Eqn. (1.1) strongly indicates of an underlying nucleation process that has been addressed by many theories^{1,10,11,12}, and primarily by Lauritzen and Hoffman. A typical barrier height for a two-dimensional nucleation (as for polymer crystallization, in which crystals do not grow in the fold-direction) goes as $1/\Delta F$, where ΔF is the free energy change per unit volume of phase change. That implies a nucleation rate of form Eqn. (1.1) (assuming a less debated proportionality between ΔF and ΔT). The Lauritzen-Hoffman theory (the LH theory) generalizes this surface nucleation concept to incorporate chain folding by proposing a distribution of crystal thickness with a cut-off minimum. The same distribution is integrated over to calculate the average thickness as an observable and to achieve the temperature dependence as in Eqn. (1.1). Sanchez and DiMarzio (the SD theory)¹¹ further considered the role of cilia (dangling chain ends) in the nucleation process, but their analysis is broadly in line with the LH theory.

To put things in perspective, it can be recalled that there are no significant barriers during the growth stage for small molecules, and the generic growth rate after initial nucleation can be expressed, based on detailed balance arguments, as:

$$G_{small} \sim g \left[1 - \exp \left(\frac{-v\Delta H \Delta T}{k_B T_c} \right) \right], \quad (1.3)$$

where, ΔH and v are, respectively, the enthalpy per unit volume and the minimum volume element of crystallization, and g is very weakly dependent on temperature. v is also involved in the factor \mathcal{P} in Eqn. (1.1) heavily affecting the growth rate. For small under-coolings ($\Delta T \rightarrow 0$) the growth rate obeys $G \sim \Delta T$ (Eqn. (1.2)), the linear relationship widely observed¹³ in small molecule crystallization and known to indicate the thermal 'roughness' regime. This behaviour of low molecular weight materials prompted Sadler and Gilmer (the SG theory) to suggest that^{14,15,16} polymer crystal growth is driven by kinetic roughening rather than nucleation. The SG theory assumed that the smallest attaching units can be fractional stems, and roughness is inevitable if the surface free energy densities are of order $k_B T_c$. This theory conceived of a barrier resulting from the interruption of growth due to pinning and subsequent removal of short stems, which are constrained by the connectivity of a longer chain. The roughness theory was hard to verify due to a lack of experimental evidence for roughening transitions¹ as most polymer crystals are observed faceted. Moreover, comparison shows that the growth rate changes by only one order of magnitude in roughness dominated growth (SG) as opposed to three in nucleation dominated growth (LH) for a typical range of super-cooling.

In addition to temperature, the other two major variables that affect polymer crystal growth significantly are polymer concentration C and polymer molecular weight M_w . The many diverse ways by which concentration and molecular weight influence the growth of polymer crystals can be summarized in the following relationship:

$$G \sim C^\gamma M_w^{-\mu} f(T_c), \quad (1.4)$$

where, a low ($\ll 1$), constant value of γ observed for high molar mass polymers lends support to barrier control at the growth front. For solution grown crystals of very low molecular weight, γ is much higher - sometimes close to or even larger than 1^{2,17}, suggesting uninterrupted diffusion-limited growth. The effective exponent μ , however, is not constant even for very low concentrations. It can assume positive or negative values depending

on the range of M_w investigated³ and is generally a complicated function of experimental variables^{18,19,20}.

Additional insight has been gained from an impressive wealth of microscopic study of the early stages of chain folding and crystal growth through Langevin dynamics simulations^{21,22,23,24,25,26,27,28,29,30,31,32} as well as Monte Carlo techniques^{33,34,35}. An overwhelming majority of simulations show accumulation of multiple polymer chains near the growth front even for very dilute solutions, especially for longer chains. This temporal congestion of molecules invokes a strong possibility that these molecules would be subject to an entropic pressure and excluded volume effect that can significantly control the growth kinetics. Polymers of low molecular weight in solution^{17,36} as well as relatively larger rigid small molecules such as GeO_2 or P_2O_5 ³⁷ follow Eqn. (1.3) suggesting that the *flexibility* of large polymer chains, not simple energy considerations, might be key to the ordering behaviour in Eqn. (1.1). Finally, many of these simulations^{33,34} and experiments do not support much variation of crystal thickness for a fixed supercooling, questioning the LH argument of a distribution and minimum of the same. Having considered these, we have developed a continuum coarse-grained theory of polymer crystallization, with a focus on the molecular details near the growth front for relatively larger chains. Mainly based on the concept of an entropic pressure, the model unifies nucleation and diffusion control behaviours as in, respectively, Eqns. (1.1) and (1.3). The key aspects of the theory are as follows. If we consider a single polymer crystal with a specific thickness, we assume that there would be accumulation of chains near the growth front resulting from an apparent nucleation control. As a result of this accumulation, which happens regardless of the bulk concentration, the local monomer concentration increases considerably, to a value (C_{in}) much higher than the rest of the system (C_0). This happens in a narrow layer region adjacent to the front (called the 'boundary layer' region henceforth)[Fig. 1]. Due to their higher concentration, these interpenetrating unadsorbed polymer chains have reduced number of configurations available that creates an entropic barrier within the boundary layer. The diffusive macromolecules must negotiate this entropic barrier before their attachment to the crystal face. The boundary values of polymer concentration C_s and C_b , respectively, at the interface ($R(t)$) and the outer boundary layer edge ($B(t)$), can be different depending on the nature of the barrier. Considering an appropriate free energy associated with the entropic barrier, and assuming the barrier layer thin enough to let the radial fluxes at the interface and the edge of the

layer be equal, the following growth rate is predicted:

$$G \sim C_0 D_{in} \exp\left(\frac{-\mathcal{P}}{T_c \Delta T}\right) [1 - \exp(-\mathcal{Q} \Delta T)], \quad (1.5)$$

where, D_{in} is the diffusivity of the polymers inside the barrier layer. \mathcal{P} and \mathcal{Q} are system variables very weakly dependent on temperature, concentration or molecular weight. Notable points on the above equation include: a) the $1/\Delta T$ factor is recovered in this theory from the proposed entropic barrier, b) the limiting behaviours of both nucleation and diffusion control are obtained in a single expression and c) the dense boundary layer enforces a dynamics different to that of the bulk system which affects the concentration and molecular weight behaviours significantly.

As an illustration of the barrier theory we numerically calculate the growth of a single crystal in dilute solution. In the numerical model, we conceive of a cylindrical lamella with circular cross-section and fixed thickness L [Fig. 2]. The fold-area dimension is typically much larger than the thickness in course of growth giving the crystal a shape like a tablet. The single crystal is embedded in a bath of diffusing polymer molecules, and during the growth process a new chain can only attach to the lateral surface, but not to the top and bottom surfaces (the fold surfaces) of the lamella. The crystal-solution interface and the edge of the boundary layer are calculated as functions of time, considering at $B(t)$ a boundary condition involving a rate-constant, which directly depends on the free energy function inside the boundary layer. The values of the effective exponents γ and μ follow from the dependencies of D_{in} and T_m on concentration and molecular weight.

The rest of the paper is organized as follows: the theory is detailed in Sec. II; the analytical and numerical results are presented in Sec. III; conclusions are summarized in Sec. IV.

II. THEORY

A. The continuity equation:

The theoretical model considers the growth of a lamella of a prescribed thickness L and the shape of a cylindrical tablet with circular cross-section (Fig. 2). The lamella grows radially outward in a medium containing polymer chains at an initial uniform concentration

C_0 . The analysis of the simplest scenario of diffusion limited growth starts with the time-dependent diffusion equation in cylindrical polar coordinates with the concentration (C) of the monomers as the diffusion variable. The azimuthal symmetry inherent in the system allows us to write,

$$D_{out} \left(\frac{\partial^2 C}{\partial r^2} + \frac{1}{r} \frac{\partial C}{\partial r} + \frac{\partial^2 C}{\partial z^2} \right) = \frac{\partial C}{\partial t}, \quad (2.1)$$

where, D_{out} is the diffusion constant and C is the concentration of the material in the outer region (all z for $r > B(t)$ and $|z| > L/2$ for $r < B(t)$). We invoke the mass balance equation at the interface ($r = R(t)$) as,

$$(C_{solid} - C_s) \frac{dR}{dt} = \text{flux at the interface}, \quad (2.2)$$

where, the concentration of monomers is C_{solid} in the crystalline (solid) phase and C_s in the uncrystallized (solution or melt) phase at the interface. $R(t)$ is the radius of the lamellar crystal as well as the location of the crystal-solution(melt) interface at time t and $B(t)$ is the location of the outer edge of the boundary layer. The growth or, in quantitative terms, the radius $R(t)$ as a function of time is calculated from Eqns. (2.1) and (2.2) which are solved in accordance with the following boundary conditions: a)

$$\frac{\partial C}{\partial n} = 0 \quad (2.3)$$

at the boundaries of the system (the container in which the crystal is growing), where, n is the direction normal to the surface; b)

$$\frac{\partial C}{\partial z} = 0 \quad (2.4)$$

at the fold surfaces (the top and bottom surfaces of the cylindrical tablet) given by $|z| = L/2$ for $0 < r < R(t)$; and c)

$$C = C_s(z) \quad (2.5)$$

at the interface layer given by $r = R(t)$ for $0 < |z| < L/2$. The reflecting boundary condition (boundary condition b)) is adopted to model the physical situation in which the polymer molecules are denied attachment to the fold surfaces of the lamella. Unlike many other theories that deal with a particle-wall type interactions³⁸, we do not assume a perfect sink boundary condition in which $C = 0$ at the wall. In our model, $C = C_s \neq 0$ at the interface

at $r = R(t)$. For crystallization at finite temperatures, desorption and the preservation of detailed balance at the interface preclude the use of a perfect sink (or an immobilizing) condition. Therefore, in general, the concentration of the mobile molecules at the interface (C_s) is an unknown variable in our theory.

To replace the boundary condition at the interface at $R(t)$ with a boundary condition at the edge of the boundary layer at $B(t)$, we start with the general expressions for the current term in diffusion equation. The generic continuity equation will be

$$\frac{\partial C}{\partial t} = \nabla \cdot \mathbf{J}, \quad (2.6)$$

where the flux \mathbf{J} is of the form

$$J_i = CV_i - D_{ij}\partial_j C + \frac{C}{k_B T} D_{ij} F_j, \quad (2.7)$$

where, i, j are indices for the components r, ϕ, z . The first term describes convection as a function of the concentration C and mass velocity V . The second term represents the driving force due to the concentration gradient, where D_{ij} are the diffusivity tensors. The third term describes an external force that can be conveniently represented by a potential or a free energy.

For the slow process of polymer crystallization, the convective current is generally negligible. Azimuthal symmetry ensures that J_ϕ must be zero. Cross diffusion is negligibly small rendering $D_{rz} = D_{zr} = 0$. In conjunction with these criteria, the standard expressions for the gradient and the divergence in cylindrical polar coordinates in Eqn. (2.7) yield the following current terms:

$$\begin{aligned} J_r &= -D_{rr}\frac{\partial C}{\partial r} + \frac{C}{k_B T} D_{rr} F_r \\ J_\phi &= 0 \\ J_z &= -D_{zz}\frac{\partial C}{\partial z} + \frac{C}{k_B T} D_{zz} F_z, \end{aligned} \quad (2.8)$$

where, the diffusivity tensor D_{ij} and the external force F_j are written in their component forms. We would be interested in steady-state growth only rendering $\frac{\partial C}{\partial t} = 0$. Combining Eqns. (2.6),(2.8) and the steady-state condition, we get

$$\begin{aligned} \nabla \cdot \mathbf{J} &= \frac{1}{r} \frac{\partial}{\partial r} \left(r \left\{ -D_{rr} \frac{\partial C}{\partial r} + \frac{C}{k_B T} D_{rr} F_r \right\} \right) + \frac{\partial}{\partial z} \left(-D_{zz} \frac{\partial C}{\partial z} + \frac{C}{k_B T} D_{zz} F_z \right) \\ &= 0. \end{aligned} \quad (2.9)$$

The analysis detailed above is a very general description of a crystallization process governed by reaction-diffusion equations (Eqn. (2.1) alongwith Eqn. (2.2)). Eqn. (2.9), although applicable to a variety of cases regardless of the size and structure of the molecules, is more appropriate for slowly diffusing linear homopolymers as mentioned above. The most challenging aspect of this scheme is to determine the concentration C_s at the interface, more so when large molecules and possible entanglements result in complex dynamics near the growth front. To deal with it in our model, we propose a method considering a dense boundary layer at the growth front, in which the polymer molecules are subject to an entropic barrier and the polymer dynamics is different than in the rest of the system. Before proceeding further with our analysis, we now provide an outline of our boundary layer formalism.

B. The boundary layer:

Schematically, we specify two different regions in the uncrystallized part of the system - namely, the 'outer region' (all z for $r > B(t)$ and $|z| > L/2$ for $r < B(t)$, Fig. 2) with the bulk polymer concentration and the 'boundary layer region' ($|z| < L/2$ for $R(t) < r < B(t)$) with concentration much higher than the bulk value. The polymer molecules are subject to free diffusion only in the 'outer region', whereas they experience entropic force inside the 'boundary layer'. These two apparently different processes are reconciled by matching the boundary conditions at the common 'interface' of these two regions ($r = B(t)$). Treatment of the boundary layer must include the effect of the free energy barrier resulting from the entropic pressure adjacent to the growth front.

Before further simplifying the expression in Eqn. (2.9), we elaborate on the assumptions made on polymer flow inside the boundary layer. If we focus on the attachment mechanism of a single polymer chain, the rectangular area at the growth front in Fig. 2 can be treated as a 'hot-seat'. Diffusing polymer molecules, while trying to attach to the growth front (or the interface at $R(t)$), would have to occupy the 'hot-seat' prior to attachment. The polymer molecules in this 'hot-seat' are subject to the entropic pressure, and therefore, our primary assumption would be the barrier force \mathbf{F} in Eqn. (2.9) is non-zero inside and negligible outside this 'hot-seat' region. In general, however, \mathbf{F} will have non-zero components F_r and F_z . We notice that, within the 'hot-seat', some of the molecules would already resemble

the structural morphology of a full grown crystal and therefore the corresponding stems will mostly be parallel to the growth front (Fig. 3a). Any diffusing molecule trying to attach from the z -direction, regardless of the orientation of its stems, will have minimal penetration within the layer (similar to the fold surfaces). Therefore, we can safely ignore F_z inside this boundary layer. Considering this and the flux in the z -direction at the mid-layer of the lamella($z = 0$) which follows

$$\frac{\partial C}{\partial z}(r, 0) = 0, \quad (2.10)$$

allowed by symmetry, we can reasonably argue that the flux in the z -direction with respect to that in r -direction can be ignored within this boundary layer region.

Instead of solving the generalized diffusion equation (Eqns. (2.6) with (2.7)) inside the boundary layer in which the barrier force \mathbf{F} is active, we propose to set up a boundary condition at the outer layer edge($r = B(t)$) as a function of relevant physical variables. Now that we have argued that the diffusion as well as the entropic force in the z -direction are negligible with respect to their r counterparts within the boundary layer, the third and fourth terms in Eqn. (2.9) may be ignored, and the steady-state continuity equation inside the layer simplifies to

$$\frac{1}{r} \frac{\partial}{\partial r} \left(r \left\{ -D_{rr} \frac{\partial C}{\partial r} + \frac{C}{k_B T} D_{rr} F_r \right\} \right) = 0. \quad (2.11)$$

As a much higher concentration inside the layer is anticipated, we set the diffusion coefficient $D_{rr} = D_{in}$, which is different from the bulk diffusivity, D_{out} . Integrating the above equation in r once, we obtain

$$r \left\{ -D_{in} \frac{\partial C}{\partial r} + \frac{C}{k_B T} D_{in} F_r \right\} = \mathcal{C}(z) \quad (2.12)$$

for $r \neq 0$. Identifying the quantity in the parenthesis as the radial flux of polymer chains $J_r(r)$, we determine the integration constant $\mathcal{C}(z)$ and express Eqn. (2.12) as

$$-D_{in} r \frac{\partial C}{\partial r} + \frac{Cr}{k_B T} D_{in} F_r = J_r|_{B(t)} B(t), \quad (2.13)$$

where, $r = B(t)$ is the edge of the boundary layer. Treating the diffusion coefficient as a general r -dependent quantity $D_{in}(r)$, multiplying by the integrating factor of form

$$\exp \left[\int_{R(t)}^{B(t)} \left[- \left(\frac{F_r(r)}{k_B T} \right) dr \right] \right]$$

and integrating once more over r , we get

$$C(r) - C_s = -J_r|_{B(t)} B(t) \exp\left(-\frac{\phi(r)}{k_B T}\right) \int_{R(t)}^{B(t)} \frac{\exp\left(\frac{\phi(r')}{k_B T}\right)}{D_{in}(r') r'} dr'. \quad (2.14)$$

Here, we have enforced the boundary condition in Eqn. (2.5). In addition, we have introduced a potential $\phi(r)$ corresponding to the force $\mathbf{F}(r)$ given by the equation

$$F_r(r') = -\frac{\partial \phi(r')}{\partial r'}. \quad (2.15)$$

Outside the boundary layer region \mathbf{F} is zero. Polymer molecules undergo free diffusion in this region and the reduced equation (Eqn. (2.9)) becomes,

$$\frac{1}{r} \frac{\partial}{\partial r} \left(-D_{rr} r \frac{\partial C}{\partial r} \right) + \frac{\partial}{\partial z} \left(-D_{zz} \frac{\partial C}{\partial z} \right) = 0. \quad (2.16)$$

Comparing with the steady state equation $\partial_i J_i = 0$, we identify the two terms in the parentheses above as fluxes in the r and z directions, respectively. Therefore, the radial flux in the outer region can be written as,

$$J_r = -D_{out} \frac{\partial C}{\partial r} \quad \text{for} \\ r \geq B(t) \quad \text{and} \quad r < B(t); |z| < L/2. \quad (2.17)$$

At this point we enforce the continuity condition at the edge of the boundary layer ($r = B(t); |z| < L/2$) for both radial flux J_r and concentration C assuming they are equal, respectively, at both sides of the boundary. Evaluating expressions valid for inside and outside of the boundary layer from Eqns. (2.14) and (2.17), respectively, and comparing them at the edge of the layer ($r = B(t)$), we obtain

$$-D_{out} \frac{\partial C}{\partial r} \Big|_{B(t)} = -\left[C(B(t)) - C_s \right] \exp\left(\frac{\phi(B(t))}{k_B T}\right) / B(t) \int_{R(t)}^{B(t)} \frac{\exp\left(\frac{\phi(r')}{k_B T}\right)}{D_{in}(r') r'} dr'. \quad (2.18)$$

Rearrangement of terms yields

$$\frac{1}{C(B(t)) - C_s} \frac{\partial C}{\partial r} \Big|_{B(t)} = K, \quad (2.19)$$

where,

$$K = \exp\left(\frac{\phi(B(t))}{k_B T}\right) / D_{out} B(t) \int_{R(t)}^{B(t)} \frac{\exp\left(\frac{\phi(r')}{k_B T}\right)}{D_{in}(r') r'} dr' \quad (2.20)$$

is conceived as the effective rate-constant for this reaction-diffusion mechanism. There are several features of the expression of K worthy of note. As suggested at the beginning of the sub-section, we have evaluated K as a function of the variables inside the boundary layer, although it can be used as a measure of the flux (Eqn. (2.19)) just at the edge of the layer. In the process of deriving K , we have eliminated all complexities of solving the full reaction-diffusion equation in the layer region ($R(t) < r < B(t); |z| < L/2$). Moreover, we have gained substantial insight into the problem just by producing a boundary condition for the bulk solution (the 'outer region') in terms of the variables inside the layer region.

C. The entropic barrier

The novel concept of a barrier created due to the accumulation of polymer molecules at the growth front is the most notable aspect in our theory. Fig. 1 illustrates the key features of the barrier. To determine this barrier quantitatively in terms of the potential $\phi(r)$, we model it with a free energy functional. The number of monomers incorporated into the solid is assumed to be roughly proportional to the distance up to which the molecule has penetrated the barrier. The polymer molecule that diffuses through the bulk, negotiates the barrier and tries to get registered in the crystal (Fig. 3) starts to feel the barrier force when at least one monomer enters the boundary layer region. It will cease to feel the force once the whole of it is incorporated into the solid. The barrier force will be maximum when roughly half of the molecule is in the solid and the other half is still in the layer region. Therefore, Gaussian or parabolic profiles (Fig. 4) for the layer free energy might be natural choices. Choosing a parabola makes the calculation easier, although the saddle-point method (described with analytical results in Section.III) illustrates that the choice has little effect on key results. The expression of the parabola in Fig. 4 would be given by

$$\phi(r) = E_h - \frac{E_h}{\left[(B(t) - R(t))/2\right]^2} \left(r - \frac{B(t)}{2}\right)^2, \quad (2.21)$$

where, E_h is the maximum height of the parabola and $\phi(r)$ is the free energy function. E_h will be identified as the barrier height henceforth.

To determine the barrier height we write the free energy in terms of the number of monomers already incorporated in the crystal (Fig. 3b) as,

$$F_m = -(N - m)\Delta F + \sigma_g \sqrt{N - m} + (1 - \gamma') \ln m, \quad (2.22)$$

where, N is the total number of monomers in the molecule, m is the number of monomers still unattached to the solid front, σ_g is a general 'surface free-energy' quantity, ΔF is the bulk energy gain per unit volume of crystallization and γ' is the surface critical exponent³⁹. Maximization of the free energy in terms of m yields,

$$F_m^* \sim \frac{1}{(\Delta F)}. \quad (2.23)$$

We identify F_m^* with E_h , the barrier height, in Eqn. (2.21) and obtain the final expression for the barrier potential,

$$\phi(r) = \frac{A}{\Delta F} - \frac{A/\Delta F}{\left[(B(t) - R(t))/2\right]^2} \left(r - \frac{B(t)}{2}\right)^2, \quad (2.24)$$

where, A is a quantity dependent on the system variables but not too sensitively dependent on temperature, concentration and molecular weight. A can be treated as a parameter in the above equation for basic growth studies that are compliant with typical experiments.

Before proceeding with our analysis, we summarize the theoretical scheme detailed above. We aimed to solve the time-dependent continuity equation (diffusion equation - Eqn. (2.1)) in the bulk polymer solution subject to the boundary conditions as specified at the wall of the container (Eqn. (2.3)), the fold surfaces of the lamella (Eqn. (2.4)) and the edge of the proposed boundary layer (Eqn. (2.19)). The monomer concentration has been treated as the diffusion variable, and the rate-constant K at the boundary layer edge is derived in Eqn. (2.20), in which the free energy functional ϕ is given by Eqn. (2.24). The growth of the interface has to be calculated from the mass-balance equation (Eqn. (2.2)) assuming that fluxes are equal at the interface and at the outer edge of the boundary layer.

III. RESULTS AND DISCUSSION

A. Analytical results:

For the above described model, it is fairly straightforward to derive the basic growth laws. The growth rate $\frac{dR}{dt}$ of the interface at $R(t)$ is given by the mass-balance equation (Eqn. (2.2)) in which the flux is calculated at the interface. On the other hand, the flux at the edge of the boundary layer at $B(t)$ is given by the boundary condition in Eqn. (2.19). Combining the two in conjunction with the major assumption above, we obtain the expression for the

growth rate G as:

$$\begin{aligned}
 G &= \frac{dR}{dt} \\
 &= D_{out} \frac{C(B(t)) - C_s}{C_{solid} - C_s} K \\
 &= D_{out} \frac{C(B(t)) - C_s}{C_{solid}} K \quad \text{for} \quad C_s \ll C_{solid}.
 \end{aligned} \tag{3.1}$$

Note that K , the rate-constant, is given by Eqn. (2.20), expanding which we obtain,

$$\begin{aligned}
 G &= \frac{dR}{dt} = D_{out} \frac{C(B(t)) - C_s}{C_{solid}} \times \exp\left(\frac{\phi(B(t))}{k_B T}\right) / \\
 &\quad D_{out} B(t) \int_{R(t)}^{B(t)} \frac{\exp\left(\frac{\phi(r')}{k_B T}\right)}{D_{in}(r') r'} dr'.
 \end{aligned} \tag{3.2}$$

Observing that $\exp[\phi_{B(t)}/k_B T]$ is a constant, we take it to be equal to 1 ($\phi_{B(t)} = 0$). We notice that D_{out} cancels (as it should always do - D_{in} is probably a linear function of D_{out}), and $D_{in}(r')$ is assumed not to vary within the boundary layer. These lead to:

$$G = D_{in} \left[B(t) \int_{R(t)}^{B(t)} \frac{\exp\left(\frac{\phi(r')}{k_B T}\right)}{r'} dr' \right]^{-1} \frac{C(B(t)) - C_s}{C_{solid}}. \tag{3.3}$$

We calculate the above integral using the saddle point approximation, in which, for any function $f(r)$,

$$\int_a^b f(r) dr = f_{max}, \tag{3.4}$$

in the leading term where, f_{max} falls in the range between a and b , and $f(r)$ dies down both toward a and b . This approximation gets better with $f(r)$ becoming narrower and steeper around $r(f_{max})$ and becomes exact when $f(r)$ is a delta function at $r(f_{max})$. With this approximation, r' has to be replaced by $(R(t) + B(t))/2$ in Eqn. (2.24). Consequently, from Eqn. (3.3) it follows that

$$G = D_{in} \frac{C(B(t)) - C_s}{C_{solid}} \frac{R(t) + B(t)}{2B(t)} \exp\left(\frac{-A}{k_B T \Delta F}\right). \tag{3.5}$$

The point worthy of note here is that we simply considered the numerator of $e^{\phi(r')/k_B T}/r'$ for the saddle-point calculation. This is valid strictly when $A/\Delta F$ is high compared to $\{B(t) - R(t)\}/R(t)$, i.e, when there is not much variation of r' with respect to the variation of the exponential function in the range between $R(t)$ and $B(t)$.

Although the above treatment is analytically sound, we still do not know the value of C_s , the concentration at the interface $R(t)$. The calculation is straightforward for temperatures low enough not to allow desorption at the growth front. In that case, $C_s = 0$, as the monomers in the polymer chain trying to attach are immobilized as soon as they come in contact with the growth front. For higher temperatures (i.e., for small super-cooling), desorption is significant, and as a consequence $C_s \neq 0$. It can be shown that the flux at finite temperatures can be written as,

$$Fl_{finite} = Fl_{zero} \left(1 - \exp \left(-\frac{v\Delta F}{k_B T} \right) \right), \quad (3.6)$$

where, Fl_{finite} and Fl_{zero} are, respectively, fluxes for a finite and zero temperatures (see, Appendix.I), and v is the volume unit that solidifies. Using the above equation and identifying Fl_{zero} as a system-specific quantity β that can be assigned a value later (Appendix.I), we immediately reach a different version for the growth law,

$$G = \beta D_{in} \frac{C(B(t))}{C_{solid}} \frac{R(t) + B(t)}{2B(t)} \exp \left(\frac{-A}{k_B T \Delta F} \right) \left[1 - \exp \left(-\frac{v\Delta F}{k_B T} \right) \right]. \quad (3.7)$$

β is a diffusion related quantity very weakly dependent on temperature. The above expression can be presented in terms of the enthalpy and the super-cooling using the relation,

$$\Delta F = \Delta H \Delta T / T_m, \quad \text{for small } \Delta T \quad (3.8)$$

where, T_m is the equilibrium melting temperature and ΔH is enthalpy per unit volume of crystallization. Doing so we obtain,

$$G = \beta D_{in} \frac{C(B(t))}{C_{solid}} \frac{R(t) + B(t)}{2B(t)} \exp \left(\frac{-AT_m}{k_B T \Delta H \Delta T} \right) \left[1 - \exp \left(-\frac{v\Delta H \Delta T}{k_B T T_m} \right) \right]. \quad (3.9)$$

This is the most important result in our analysis. We have taken the liberty of applying Eqn. (3.8) for finite molecular weights also, although it is almost unquestionably valid in the infinite molecular weight limit only. The volume element v is substantial for large molecules because it depends on the smallest attaching element to which the attachment-detachment rate-constants can be assigned. With a polymer chain, it is an involved analysis¹ to determine whether the incorporation of a stem is a one-step process or not. In our theory, we have treated v as a parameter that is believed to be of a value endorsed by experiments. We note

that the above expression for the growth rate G does not involve any unknown variable from inside the boundary layer region. Further, it incorporates the factor of the detailed balance which is present regardless of the size of the molecule. The $\exp\left(\frac{-A'}{T\Delta T}\right)$ factor, in addition to the detailed balance factor, has most abundantly been observed in all sorts of nucleation dominated growth phenomena. As shown above, this factor is recovered in our analysis by using the boundary layer approach in which it is embedded in the rate-constant K .

In the special case of a dilute solution, the concentration at the boundary layer edge, $C(B(t))$, is proportional to the initial bulk concentration C_0 , and so is the concentration inside the layer. Physically, both the width of the boundary layer ($B(t) - R(t)$) and the diffusion constant inside the layer (D_{in}) will depend on the concentration of the solution. For higher concentrations, the polymer molecules will entangle to a higher degree near the growth interface. As a result, the range of the entropic-barrier which originates from this entanglement would be larger making the boundary layer thicker. The self-diffusivity inside the boundary layer will also decrease with increasing C . We assume the conventional theory⁴⁰ of power-law dependence of the self-diffusivity D_{in} on concentration of the form

$$D_{in} \sim \frac{1}{C^\alpha}, \quad (3.10)$$

where α is a positive number, to be valid inside the layer. Using this relation and the argument above, the growth rate in Eqn. (3.9) can be written as,

$$G \sim C^{1-\alpha} \equiv C^\gamma, \quad (3.11)$$

where, γ is the concentration exponent. Note that we have left the barrier height E_h as well as the parameter A in the expression of growth rate (Eqn. (3.9)) as independent of concentration.

B. Numerical results:

In the previous subsection we discussed the aspects of a continuum theory describing the reaction-limited regime of polymer crystallization and analytically derived the growth laws for a general case of solutions as well as melts. In this sub-section, we present numerical calculations for the specific case of dilute solutions to corroborate the analytical theory. In the numerical treatment, we address a much wider range of physical situations. As

mentioned before, even without considering the complicated barrier forces, the exact solution of the problem involving a moving boundary is analytically untractable for this circular cylindrical geometry. Numerical solution is not only capable of dealing with very complicated entropic barriers and higher degrees of diffusion in different geometries, but also does allow us to analyze competing effects resulting from the variation of a single parameter, e.g., the molecular weight. For example, as the molecular weight increases, at one hand it increases the effective super-cooling and hence the growth-rate but on the other hand, it enhances the barrier-effect that impedes the growth. Numerical calculations deliver the results in a more compact form in these scenarios in which no single exponent (μ in Eqn. (1.4)) exists for the whole range of the parameter (molecular weight) investigated.

The essence of our numerics is as follows: we have solved the diffusion equation (Eqn. (2.1)) in the region enclosed by the boundary layer at $B(t)$, the fold surfaces and the walls of the container (Fig. 2), subject to the reflective boundary conditions (Eqns. (2.3), (2.4)) and the modified mass-balance condition (Eqn. (2.19)). The rate constant K (Eqn. (2.20)) is determined at each step as a function of the diffusion constant, the range of the barrier and the form of the free energy functional related to the barrier interaction force. Numerically, we fix the initial radius $R(t = 0)$ at the beginning of the iteration. The rate-constant K is calculated subsequently at $B(t = 0)$. The flux at the edge of the boundary layer ($B(t)$) at finite temperatures is calculated from a formula related to the flux at zero temperature (or a very low temperature - for details of this method see Appendix.I). The fluxes at the edge of the boundary layer ($B(t)$) and at the interface ($R(t)$) are equated (or, at the least, made proportional) Once the concentration (C) for the whole space in the bulk solution is updated, the new radius is calculated from the old radius using the mass balance equation (Eqn. (2.2)). Note that a rigorous integration in Eqn. (2.20), instead of a saddle-point approximation, is possible in the numerical scheme.

There is an important aspect in the simulation that warrants a note. The growth of a single crystal in a dilute solution involves a moving boundary in a time-dependent diffusive environment. These problems are generally treated as moving boundary value problems in the literature. Till date, there is no analytical solution available for this problem in a finite circular cylindrical system with arbitrary concentrations as the diffusion variable. In our numerical program, we have employed a technique in which the position-grid in the radial direction (r values) has been adjusted at each step so that one grid-point always coincides

with the edge of the boundary-layer, at which location the rate constant boundary condition (Eqn. (2.19)) is enforced.

As mentioned before, three major factors affecting the growth rate and typically discussed in the literature have been investigated in our numerical work on dilute solutions. They are the crystallization temperature T_c (in terms of the under-cooling or super-cooling ΔT) of the system, concentration (C) of the bulk solution and the molecular weight (M_w) of the crystallizing polymer. Polymer crystallization typically being a very slow process no temperature gradient is assumed to be present in the solution.

1. Under-cooling, ΔT :

Linear homopolymers in a dilute solution are generally crystallized by reducing the temperature below the equilibrium melting temperature or, in other words, by undercooling the solution. Experiments throughout have shown that the growth rate depends heavily on the degree of under-cooling, and it has been orders of magnitude lower than what is expected in a diffusion limited growth. At the same time, it has been observed that the rate changes by orders of magnitude for a relatively small change in temperature. All these evidences strongly suggest that polymer crystal growth in dilute solutions is a reaction-dominated phenomena, the reaction at the growth face being critically dependent on the degree of under-cooling ΔT .

The saddle-point analysis in the last section had shown that the growth rate can be written as

$$G \sim C_0^\gamma \exp^{-(A'/T_c \Delta T)} \left[1 - \exp^{-(B' \Delta T)} \right], \quad (3.12)$$

where, T_c is the crystallization temperature, A' and B' are system parameters not too critically dependent on temperature, concentration or molecular weight, C_0 is the initial concentration, γ is the concentration exponent and $\Delta T = T_m - T_c$, where, T_m is the equilibrium melting temperature of that specific polymer. We did an explicit numerical calculation of the growth rate for three different concentrations, $C = 0.01$, 0.001 and 0.0001 , all of which fall in the dilute regime. The growth rate G is plotted against the factor $1/T_c \Delta T$ in Fig. 5. The temperature range considered was from 15 degree to 25 degree below T_m . Comparing this result with experiments by Keller and Pedemonte², we infer that our theory has

excellent compliance with the generic experimental results as the graphs are good straight lines with the growth rate increasing by at least three orders of magnitude for an increase in undercooling from 15 to 25 degrees. As expected, the slope of the straight lines remain unaltered for all concentrations implying no dependence of concentration on the prefactors A' and possibly B' . The numerical result corroborates the well-known experimental observation that the nucleation factor entirely suppresses the detailed balance factor (Eqn. (3.12)) for the given range of moderate under-coolings.

To compare the above mentioned growth governed by nucleation and entropic barrier to one that is not (and hence allows uninhibited diffusion-limited attachment), we calculated crystal growth for very large values of both the rate-constant K (implying effectively zero barrier) and under-cooling ΔT (implying no dissolution). The rate-constant in these calculations is fixed externally and does not depend on the under-cooling. The growth rate is plotted for four different diffusivities in Fig. 6a. A sufficiently long time-range of the growth inside the container has been captured, and hence it shows the effect of depletion of available material during the later part of the growth. The initial growth rate, free from the effect of the finite boundary, is found to be orders of magnitude higher than the nucleation dominated rates in Fig. 5. To show the effect of the barrier, we have performed similar growth calculations for lower values of K and plotted the growth (R) with time (t) in Fig. 6b. We notice that the growth rate saturates to the value corresponding to diffusion-control for high values of K . We further calculated the growth for small under-coolings ($\Delta T = 5$ to 20 degrees) and plotted it (R) with time (t) in Fig. 6c. It is evident from the plot that the effect of desorption, which is a significant fraction of adsorption at moderate under-coolings, slows down the process. But, as we notice from the slopes of the four curves in Fig. 6c, the growth rate changes by only a factor of two for a 10 degree change in under-cooling. This is way less than the factor of 10^3 present in the nucleation dominated growth in Fig. 5.

2. Concentration, C :

In case of diffusion limited growth for small molecules in a solution, the growth rate is generally proportional to concentration. The fact that the growth rate depends on concentration raised to the power some number less than unity implies the presence at the growth front of a barrier, the strength of which depends on the concentration itself. In mathematical

terms, γ in

$$G \sim C^\gamma \quad (3.13)$$

has been observed to be less than one in most cases^{2,3}.

As per the analytical discussion in section III.A, Eqn. (2.2) and Eqn. (2.19) can be simplified to show that the growth rate follows

$$\begin{aligned} G &\sim \text{flux} \\ &\sim D_{out} \frac{\partial C}{\partial r} \\ &\sim D_{out} K C, \end{aligned} \quad (3.14)$$

where we have left out the temperature factors for the time-being (see, Eqn. (3.12)). For generic linear homopolymers in solution, the dissolution temperature T_d does not vary much with concentration, especially in the higher molecular weight limit (a specific example of polyethylene in xylene is given in⁴³). Therefore, the equation above implies that unless the rate-constant K is a function of C , the growth rate is simply proportional to it and γ is unity. For small molecules, K is unaffected by the concentration of the solution, but for molecules as large as polymers, we suggest that the concentration has an effect on the degree of crowding of molecules at the growth front, and hence it affects the value of K . A simplified version of Eqn. (2.20) sheds more light on the effect of various quantities, especially concentration, on the growth rate (section III.A). Considering the concentration dependence of the self-diffusivity inside the boundary layer region, a simple dependence of growth rate on concentration has already been obtained (Eqns. (3.10) and (3.11)) in this article. In the dilute solution limit - for example for polystyrene polymer in benzene with the initial concentration being less than 0.01 - α is close to zero and the self-diffusivity D_{in} does not vary much with the density of monomers⁴¹. On the other hand, if the concentration is close to 0.1 or higher, the Rouse regime sets in and α is close to 2. In our model, we expect the concentration inside the layer to be somewhere in this range, and hence the value of α to be between 0 and 2, with the most probable values being around 0.5 to 1. For example, if we take the value of α to be 0.5, γ is 0.5 which is an acceptable result supported by experiments^{2,3}. For many experiments in higher concentrations, γ has been found to be very low (0.1 to 0.2). However, if we notice that $\gamma = 1 - \alpha$ in Eqn. (3.11), it is apparent that the value of α , depending on the concentration of the solution would affect the growth rate

in a very simple but significant way. Assumption that the concentration inside the barrier layer renders α to be close to but little less than unity immediately results in a growth rate highly insensitive to concentration. The data in Ref.⁴¹ is very much supportive of the above hypothesis. To obtain a wider range for the value of γ as observed in experiments, one has to consider other factors as mentioned above, which, at this point, are beyond the scope of this work.

The growth rate as a function of concentration is plotted for two under-coolings in Fig. 7. The higher growth-rate (dashed) line is for higher under-cooling ($\Delta T = 25$) and the lower (solid) line is for lower under-cooling ($\Delta T = 15$). The value of α used in Eqn. (3.11) is 0.5. No dependence of growth rate on the crystallization temperature (T_c) has been observed. The value of the concentration exponent γ is found to be 0.5 in both cases.

3. Molecular weight, M_w :

Unlike temperature and concentration, the molecular weight affects the growth rate non-monotonically as it is almost impossible to find one single molecular weight exponent for the whole range of it. Assuming all other things remain the same, the growth rate depends on concentration with a fixed exponent. This is applicable for a good range of concentration large and small molecule systems alike because of the diffusion control which is proportional to C . A change in molecular weight for flexible macromolecules, however, changes their equilibrium melting temperature (T_m), and hence changes the effective super-cooling ($\Delta T = T_m - T_c$) when experiments are performed on an isotherm (T_c). This change in ΔT is not linear with M_w and, therefore, is the specific reason behind the non-monotonic molecular weight dependence (logarithmic) of the growth rate. In light of our theory, the other major effect we propose is that increasing molecular weight decreases the self-diffusion constant D_{in} inside the boundary layer slowing down the growth rate. These two competing effects render the molecular weight dependence of the growth rate to be complicated and analytically complex. In a typical system, for example for polyethylene single crystals in xylene solution, the growth rate increases with the molecular weight for small M_w 's and later hits a plateau or even decreases for higher M_w 's depending on the concentration of the solution.

To numerically calculate the growth rates as a function of the size of the molecule, we use the well-known empirical expression for the equilibrium melting temperature as a function

of the molecular weight. The melting or dissolution temperature of a finite molecular weight polymer can be written as⁴²,

$$T_m = T_m^0 - \frac{E}{M_w}, \quad (3.15)$$

where, T_m^0 is the equilibrium melting temperature for infinite molecular weight and E is a constant for the polymers of the same series with different molar mass. The above formula is a Gibbs-Thomson type expression relating the melting temperature for finite and infinite systems but is still phenomenological, and input for E must be obtained from real systems. T_m^0 and E are available for several systems in the literature^{42,43}. To account for the other effect, in accordance with the conventional polymer theories, the following dependence of the self-diffusion constant D_{in} on the molecular weight can be assumed:

$$D_{in} \sim \frac{1}{M_w^x}, \quad (3.16)$$

where, x is unity in the Rouse regime. We can predict the trend of the growth rate versus molecular weight curve qualitatively from above two relations. For low molecular weights, a change in T_m (hence ΔT , the effective super-cooling) with M_w will be significant implying large change in the growth rate due to the $\exp[-1/T_c \Delta T]$ factor. The growth rate would, therefore, increase rapidly with M_w in the lower range. For larger molecular weights, T_m will saturate to the value of T_m^0 . If M_w is further increased, Eqn. (3.15) will cease to affect the rate and Eqn. (3.16) will take over. The growth mechanism, therefore, will be progressively retarded. The curve might have a plateau depending on the constants involved in the above two equations.

Using the relationships mentioned above in our numerics, we have plotted the growth rate (G) against the molecular weight (M_w) for three crystallization temperatures ($T_c = T_m^0 - 25, T_m^0 - 30, T_m^0 - 35$) (Fig. 8). The rate-curve isotherms agree reasonably well with the qualitative argument presented above and with experiments³. We have chosen the concentration C to be 0.001, which is at the middle of the range we considered in this work. The shapes of the isotherms do not change significantly with concentration, although the absolute values of the growth rates do. There are no plateau in these particular curves but various forms and shapes of these isotherms are obtained in our numerics by changing the constants, especially E , as mentioned above.

The effect of the molar mass of the polymers on the concentration exponent γ has been investigated extensively³ in the literature and is worthy of analysis. For a substantial range

of crystallization temperatures, γ goes down with M_w for a fixed crystallization temperature, T_c . In other words, the effect that renders the growth rate more insensitive to concentration increases with the molecular weight of the polymer. Within the purview of our theory, this implies of two possibilities: a) the self diffusion constant D_{in} inside the barrier layer still follows Eqn. (3.10) but α increases with M_w and b) the range of the barrier layer ($R(t) < r < B(t)$), and therefore, the limit of integration in the expression of the rate constant K (Eqn. (2.20)), has a concentration dependence of the form $\sim C_0^y$, where, y increases with M_w . Either of the effects or both can be present. Once this hypothesis is proved to be valid, one might reproduce the growth rate versus molecular weight curves at different isotherms for different concentrations³ and show that growth becomes more inhibited for higher concentrations for the same range of molecular weight. At this point, this analysis is in a speculative level and we refrain from making a conclusive remark on this.

IV. CONCLUSIONS

The key conclusion reached from our theoretical formalism is that the flexibility or conformational entropy of the polymer chains is the distinctive rate-controlling factor that separates polymer crystallization from small-molecule crystallization. There is a significant entropic contribution to the free energy ($E - TS$) of the ordering process due to the reduction of available conformations of the polymer chains. The barrier layer theory we propose addresses the entropy factor in addition to the energy factor, which is the only factor the LH theory and its modifications consider. This formalism recovers both the nucleation dominated limit for large flexible molecules (Eqn. (1.1)) and diffusion controlled limit for small molecules (Eqn. (1.3)) in one single expression. In addition, unlike in the LH theory, this model considers one fixed thickness and still recovers the ' $\exp(-1/T\Delta T)$ ' factor most abundantly observed in polymer crystallization literature.

The free energy barrier related to the loss of entropy is assumed to be prevalent in a narrow layer adjacent to the growth front, referred to as the barrier layer or the growth zone. The temporal congestion of entangled chains occurs only in this region creating an impedance to the lateral growth process. The conclusive analytical result in our theory is

summarized in the following expression:

$$G \sim C_0 D_{in} \exp(-\mathcal{P}/T_c \Delta T) [1 - \exp(\Delta H \Delta T / k_B T_m T_c)], \quad (4.1)$$

where, G is the linear growth rate, C_0 is the initial concentration, D_{in} is the diffusion coefficient inside the boundary layer, ΔH is the enthalpy of fusion, ΔT is the under-cooling, T_m is the melting temperature at the finite molecular weight, T_c is the crystallization temperature and \mathcal{P} is a parameter which depends on the details of the entropic barrier as well as on ΔH , T_m and T_c . The above equation captures both the barrier control ($G \sim \exp(-1/\Delta T)$) and diffusion control ($G \sim \Delta T$, for small ΔT). Both D_{in} and the ' $\exp(-1/T_c \Delta T)$ ' term become insignificant when the barrier layer thickness is negligible, i. e., for low molecular weight polymers in solutions and small molecules.

Physical variables such as the diffusivity and its dependency on concentration and molecular weight have been assumed to follow a different dynamics in the dense growth zone. Following this, the above growth law predicted growth rates to be weakly or marginally dependent on concentration (the exponent γ in $G \sim C^\gamma$ is $<$ or $\ll 1$, respectively). These agree well with the experimental results which at the very first place suggested a barrier control near the growth front. In addition, considering a phenomenological relation between the melting temperature and molecular weight, we recovered typical experimental results for the dependency of growth rates on molar mass.

Our formalism is qualitatively different from the classical formulations of polymer crystallizations based only on energy arguments. Although the flexible nature of long chain molecules gives rise to various complex and diverse growth forms, we have shown that the growth can be modelled by simple physical processes considering a few typical features of crystallization. However, more detailed work is needed to determine the true nature of the entropic barrier, and to make quantitative comparison with experiments.

A few observations related to our work are noteworthy. First, we have retained the concept of a surface free energy for the crystal-liquid interface assuming the basic arguments for the origination of the energy to be still valid. The degeneracy due to many possible and energetically equivalent options for the stems to arrange themselves on the surface gives rise to the surface free energy at the very first place. In our model, the stems are still subject to this degeneracy *at* the front after they negotiate the entropic barrier layer *adjacent* to the

front.

Second, we turn our attention to the important parameter \mathcal{P} in Eqn. (4.1). This parameter has a direct correlation to the minimum volume unit v that solidifies in 'near equilibrium' (the detailed balance factor). Therefore, A contains the thickness, l , of the growing lamella. It might be possible to formulate the effect of quench depth ΔT on the thickness, broadly in line with the traditional theories. Our theory, however, has shown that a thickness dependent growth rate is not a necessary prerequisite to generate the 'nucleation' factor (see also Appendix.II).

Third, for a fixed molecular weight M_w , the concentration exponent γ has been observed in experiments to increase slightly with T_c , the crystallization temperature. We did not address this behaviour in our theory.

ACKNOWLEDGMENT

Financial support for this work was provided by the National Science Foundation Grant DMR-0605833 and MRSEC at the University of Massachusetts, Amherst.

REFERENCES

-
- ¹ K. Armitstead and G. Goldbeck-Wood, Adv. Polym. Sci. **100**, 219 (1992) and references therein.
 - ² A. Keller and E. Pedemonte, J. Cryst. Gr. **18**, 111 (1973).
 - ³ M. Cooper and R. St. J. Manley, Macromolecules **8**, 219 (1975).
 - ⁴ A. Toda, Polymer **28**, 1645 (1987).
 - ⁵ J. Langer, Rev. Mod. Phys. **52**(1), 1 (1980).
 - ⁶ A. Dougherty and J. P. Gollub, Phys. Rev. A **38**, 3043 (1988).
 - ⁷ A. J. Malkin et al., Phys. Rev. Lett. **75**, 2778 (1995).
 - ⁸ J. C. LaCombe, M. B. Koss and M. E. Glicksman, Phys. Rev. Lett. **83**, 2997 (1999).
 - ⁹ J. Deutscher and Y. Lereah, Phys. Rev. Lett. **60**, 1510 (1988).
 - ¹⁰ J. D. Hoffman, G. T. Davies, J. I. Lauritzen in N. B. Hanay(ed) *Treatise on solid-state chemistry*, Vol.3 (Plenum, New York, 1976, p 497).

- ¹¹ I. C. Sanchez and E. A. DiMarzio, J. Chem. Phys. **55**, 893 (1971).
- ¹² F. C. Frank and M. Tosi, Proc. Roy. Soc. **263**, 1314, 323 (1961).
- ¹³ G. H. Gilmer, K. A. Jackson in E. Kaldis and H. J. Scheel(ed) *Crystal growth and materials* (North Holland, Amsterdam, 1977).
- ¹⁴ D. M. Sadler, Polymer **24**, 1401 (1983).
- ¹⁵ D. M. Sadler, Polymer **28**, 1440 (1987).
- ¹⁶ D. M. Sadler and G. H. Gilmer, Polymer **25**, 1446 (1984).
- ¹⁷ J. Zhang and M. Muthukumar, preprint and personal communication.
- ¹⁸ S. Umemoto et al. , J. Macro. Sc., Part B **B42**(3-4), 421 (2003).
- ¹⁹ S. Umemoto, N. Kobayashi and N. Okui, J. Macro. Sc., Part B **B41**(4-6), 923 (2002).
- ²⁰ S. Umemoto and N. Okui, Polymer **46**, 8790 (2005).
- ²¹ M. Muthukumar, J. Chem. Phys. **104**, 691 (1996).
- ²² T. A. Kavassalis and P. R. Sundararajan, Macromolecules **26**, 4144 (1993).
- ²³ C. Liu and M. Muthukumar, J. Chem. Phys. **109**, 2536 (1998).
- ²⁴ S. Fujiwara and T. Sato, Phys. Rev. Lett. **80**, 991 (1998).
- ²⁵ M. Muthukumar, Eur. Phys. J. E **3**, 199 (2000).
- ²⁶ M. Muthukumar and P. Welch, Polymer **41**, 8833 (2000).
- ²⁷ P. Welch and M. Muthukumar, Phys. Rev. Lett. **87**, 218302 (2001).
- ²⁸ T. Yamamoto, J. Chem. Phys. **115**, 8675 (2001).
- ²⁹ I. Dukovski and M. Muthukumar, J. Chem. Phys. **118**, 6648 (2003).
- ³⁰ M. Muthukumar, Phil. Trans. R. Soc. Lond. A **361**, 539 (2003).
- ³¹ M. Muthukumar, Adv. Chem. Phys. **128**, 1 (2004).
- ³² T. Yamamoto, Polymer **45**, 1357 (2004).
- ³³ J. P. K. Doye and D. Frenkel, J. Chem. Phys. **110**, 2692 (1999).
- ³⁴ J. P. K. Doye, Polymer **41**, 8857 (2000).
- ³⁵ J.-U Sommer and G. Reiter, J. Chem. Phys. **112**, 4384 (2000).
- ³⁶ M. Muthukumar, in *Progress in understanding of Polymer Crystallization*, Editors: G. reiter and J. U. Sommer. (Lect. Notes Phys. **714**, 1 (2007)) (Springer-Verlag Berlin Heidelberg 2007).
- ³⁷ B. Wunderlich, Fig. VIII.2, *Macromolecular Physics, Vol.3* (Academic Press, New York, 1980).
- ³⁸ M. R. Myers, C. D. Lytle and L. B. Routson, Bul. Math. Biol. **61**, 113-140 (1999).
- ³⁹ M. Muthukumar, J. Chem. Phys. **111**, 10371 (1999).

- ⁴⁰ M. Doi, *Introduction to Polymer Physics* (Clarendon Press, Oxford, 1996).
- ⁴¹ H. Hervet, L. Leger and F. Rondelez, Phys. Rev. Lett. **42**, 1681 (1979).
- ⁴² B. Wunderlich, *Macromolecular Physics, Vol.3* (Academic Press, New York, 1980).
- ⁴³ E. Passaglia and F. Khoury, Polymer **25**, 631 (1984).

APPENDIX.I

In this section we present a simple derivation for the expression of particle flux at the growth front at finite temperatures (as described in Sec.III). As desorption is important at a finite temperature situation, we consider the inward and the outward fluxes separately and the difference is the net flux of particles that finally attach to the growing surface. Representing the inward and outward fluxes as Fl_{in} and Fl_{out} , respectively, and assuming the detailed balance to be valid at the interface, we write,

$$\frac{Fl_{out}}{Fl_{in}} = \exp\left(-\frac{v\Delta F}{k_B T}\right), \quad (5.1)$$

where, ΔF is the gain in free energy per unit volume after solidification and v is the volume unit that solidifies. ΔF is, in general, proportional to super-cooling ΔT for small ΔT 's and diverges with ΔT . Assuming the fluxes Fl_{in} and Fl_{out} to be $\beta e^{-F_1/K_B T}$ and $\beta e^{-F_2/K_B T}$, respectively, where, F_1 and F_2 are the activation energies for attachment and detachment, respectively, and assuming β to be an arbitrary, temperature independent quantity, we can express the net flux, $Fl_{total} = Fl_{in} - Fl_{out}$, at the interface as

$$Fl_{total} \equiv \left.\frac{\partial C}{\partial r}\right|_{r=R(t)} = \beta \left(1 - \exp\left(-\frac{v\Delta F}{k_B T}\right)\right). \quad (5.2)$$

For $\Delta T \rightarrow \infty$ (at very low temperatures) the rate of desorption at the interface is negligible to the rate of absorption and almost all the molecules that attach to the interface stick there permanently to be a part of the full-grown crystal. In this limit, the perfect sink boundary condition ($C = 0$) applies at the interface because all the diffusing molecules are immobilized as soon as they come in contact with it. This implies that

$$\beta = \left.\frac{\partial C}{\partial r}\right|_{r=R(t), C_s=0}. \quad (5.3)$$

The factor $e^{-F_1/K_B T}$ in Fl_{in} is very weakly dependent on temperature can be assumed to be a constant for a moderate range of temperature. Considering that and combining

Eqns. (5.2) and (5.3) we reach a general expression for the flux at the interface at finite temperatures,

$$\begin{aligned} & \left. \frac{\partial C}{\partial r} \right|_{r=R(t), \text{general}} \\ &= \left. \frac{\partial C}{\partial r} \right|_{r=R(t), C_s=0} \left(1 - \exp \left(-\frac{v\Delta F}{k_B T} \right) \right), \end{aligned} \quad (5.4)$$

which is applied in the algorithm described in Sec.III.

APPENDIX.II

In this section we derive the growth rates for different regimes using a fundamental surface nucleation theory and compare the results with that of the Lauritzen-Hoffman theory. The theory presented here is much simpler and does not require to conceive a cut-off minimum and a distribution of thickness as in the LH theory. We start with the basic expression for the free-energy change for solidification of m number of stems of width (the lateral direction of 'substrate completion') a , thickness (the growth direction normal to the interface) b and length (lamellar thickness) l . The free energy consists of the conventional bulk gain and surface loss terms and we have

$$\Delta G = -mabl\Delta F + 2bl\sigma + 2mab\sigma_e, \quad (6.1)$$

where, σ and σ_e are the lateral and fold surface free energies, respectively. To determine the critical free energy $(\Delta G)^*$, the expression in Eqn. (6.1) is maximized with respect to both variables in the system - the number of stems in a nucleus m and the thickness of the lamella l . Consequently, $\partial\Delta G/\partial m = 0$ and $\partial\Delta G/\partial l = 0$ imply, respectively, that

$$\begin{aligned} l^* &= \frac{2\sigma_e}{\Delta F} \quad \text{and} \\ m^* &= \frac{2\sigma}{a\Delta F}, \end{aligned} \quad (6.2)$$

where, l^* and m^* denote the critical values (at $(\Delta G)^*$) for the quantities. Substituting the critical values in the expression of ΔG , we obtain

$$(\Delta G)^* = \frac{4\sigma\sigma_e b}{\Delta F}, \quad (6.3)$$

which has been the essential conclusion for the LH theory. To illustrate the comparison we recall that for the small molecule nucleation theory, the growth rate G_r is a function of the

nucleation rate i , which in turn depends on the height of the nucleation barrier $((\Delta G)^*$ in our case) in the following way,

$$i \sim \exp \left(-\frac{(\Delta G)^*}{k_B T} \right). \quad (6.4)$$

Substitution of the expression for $(\Delta G)^*$ (Eqn.6.3) in the above equation yields,

$$i \sim \exp \left(-\frac{4\sigma\sigma_e b}{\Delta F k_B T} \right), \quad (6.5)$$

which is the more well-known LH result. The regime I and II expressions can be obtained following the arguments in line with the standard nucleation theories. For the two-dimensional geometry of polymer crystal growth, in regime I, the growth rate $G_r \sim i$ and in regime II, $G_r \sim i^{1/2}$. In conjunction with the expression for the nucleation rate i and assuming that the analysis is tenable to large molecules, the growth rates immediately explain the slope change of the $\log G$ vs. $1/T_c \Delta T$ straightline by a factor of two when the growth process shifts from regime I to II.

FIGURE CAPTION

Fig. 1.: Concentration (C) and free energy (ϕ) profiles as a functions of the distance from the interface (r). Polymer molecules accumulate (top) in the boundary layer region, the concentration increases substantially (the graph is not to scale - C is order of magnitude higher in the layer region) close to the interface (middle) and a free energy related to the entropic barrier is created (bottom) near the interface.

Fig. 2.: Schematic of the tabular growth of polymer crystals from dilute solution. Flat surfaces of the right circular cylinder normal to z axis are the fold surfaces with no growth. The solid-solution interface is at $R(t)$ and the edge of the dense boundary layer is at $B(t)$.

Fig. 3.: Schematic of the chain attachment and the related free energy: (top) different stages of attachment of one single chain to the growth front. (bottom) the free energy as a function of the number of monomers attached. There is a critical number above which the process is downhill.

Fig. 4.: A model free energy barrier as a function of the distance from the interface. The shape is chosen as a parabola in the theory.

Fig. 5.: The temperature dependence of growth plotted as growth rate (G) vs. $1/(T_c\Delta T)$ for three concentrations: $C = 0.0001$ (plus), $C = 0.001$ (diamond), $C = 0.0001$ (circle). In the log-scale they are excellent straight lines for all three concentrations. The abscissa is multiplied by 10^5 and the ordinate has arbitrary units.

Fig. 6.: Growth or size (radius R) as a function of time t in various conditions: (a) diffusive with no barrier (rate constant K is very high) and at a very high super-cooling ΔT (no dissolution) for diffusion co-efficients (D): 0.01, 0.05, 0.10, 0.15. (b) at a very high super-cooling ΔT (no dissolution) for various barrier strengths: $K = 0.1, 1, 10, 1000$ with $D = 0.1$. Notice that the growth rate saturates with increasing K . (c) for a fixed barrier strength ($K = 1.0$) and diffusion co-efficient ($D = 0.1$) for various moderate super-coolings, $\Delta T : 5, 10, 15, 20$. Dissolution is significant at these super-coolings. Depletion of material is reflected as the graphs flatten for long times. Graph (c) indicates that, for cases where K is not dependent on ΔT , growth rate changes by less than one order for a typical experimental range of ΔT .

Fig. 7.: The concentration dependence of growth plotted as growth rate (G) vs. concentration (C) for two super-coolings: $\Delta T = 15$ (circles), $\Delta T = 25$ (diamonds). In the log-scale they are excellent straight lines with slope (γ) being close to 0.5 for both ΔT . No dependence on the crystallization temperature, T_c , is allowed in the theory.

Fig. 8.: The molecular weight dependence of growth plotted as growth rate (G) vs. (M_w) for three crystallization temperatures: $T_c = T_m^0 - 25$ (circles), $T_c = T_m^0 - 30$ (squares), and $T_c = T_m^0 - 35$ (diamonds). T_m^0 is the equilibrium melting temperature in the infinite molecular weight limit. The concentration is chosen to be $C = 0.001$. We notice that there is no fixed molecular weight exponent for the growth for the entire range of M_w . In fact, generally, the growth rate increases with M_w initially (due to the increase of effective super-cooling) and decreases later (due to the entropic force near the barrier).

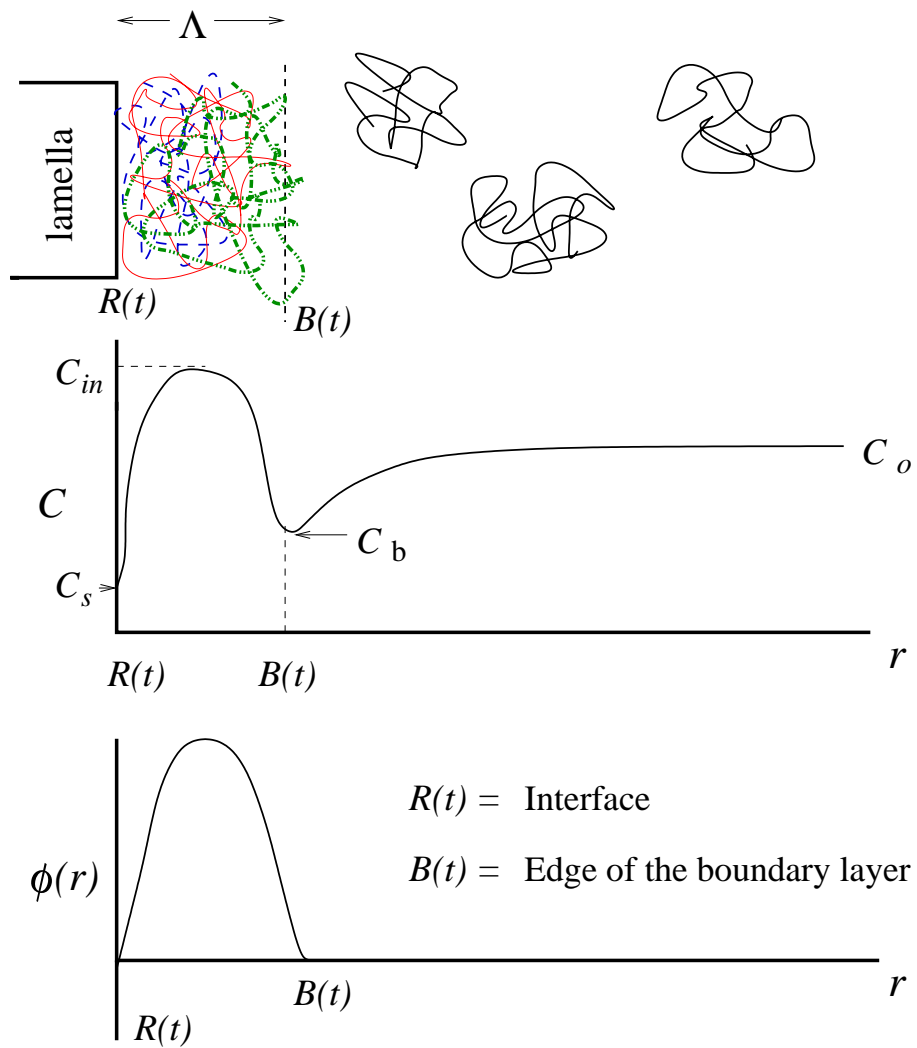


FIG. 1: Kundagrami *et al.*, *JCP*

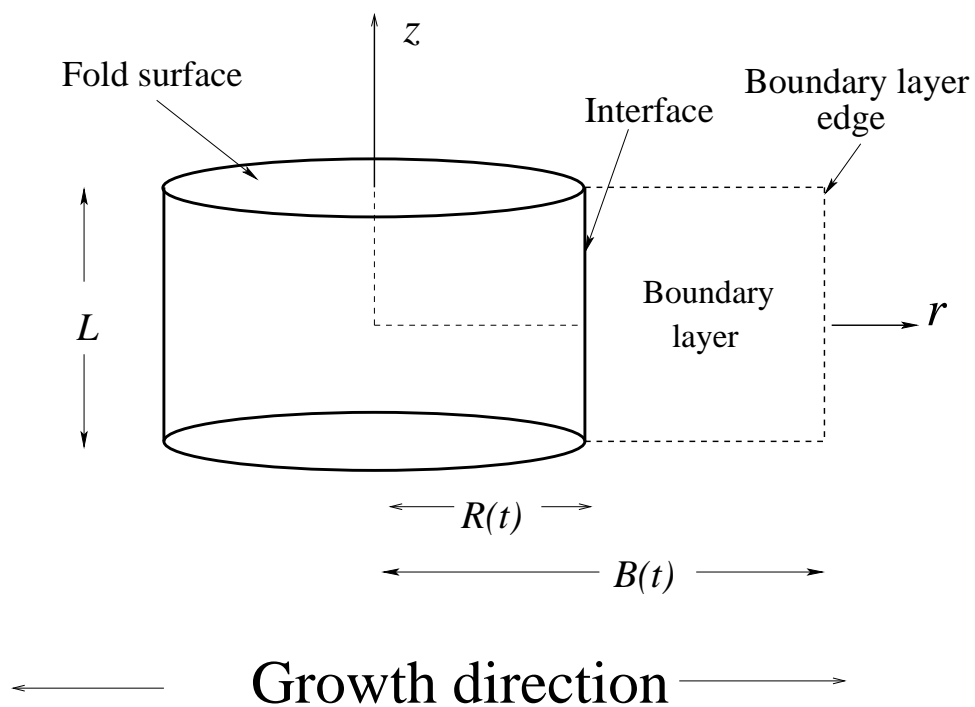


FIG. 2: Kundagrami *et al.*, *JCP*

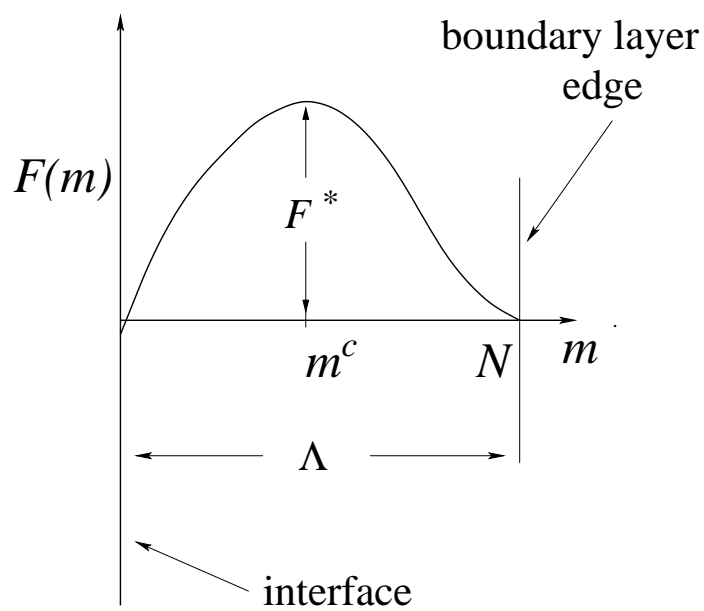
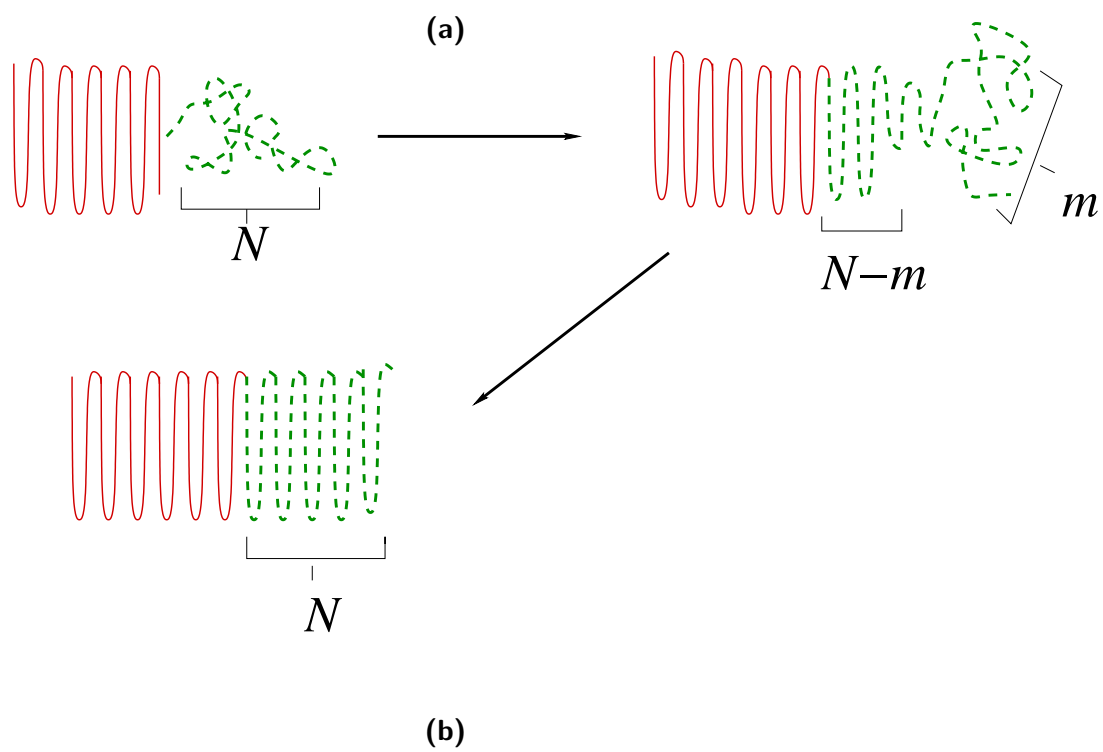


FIG. 3: Kundagrami *et al.*, *JCP*

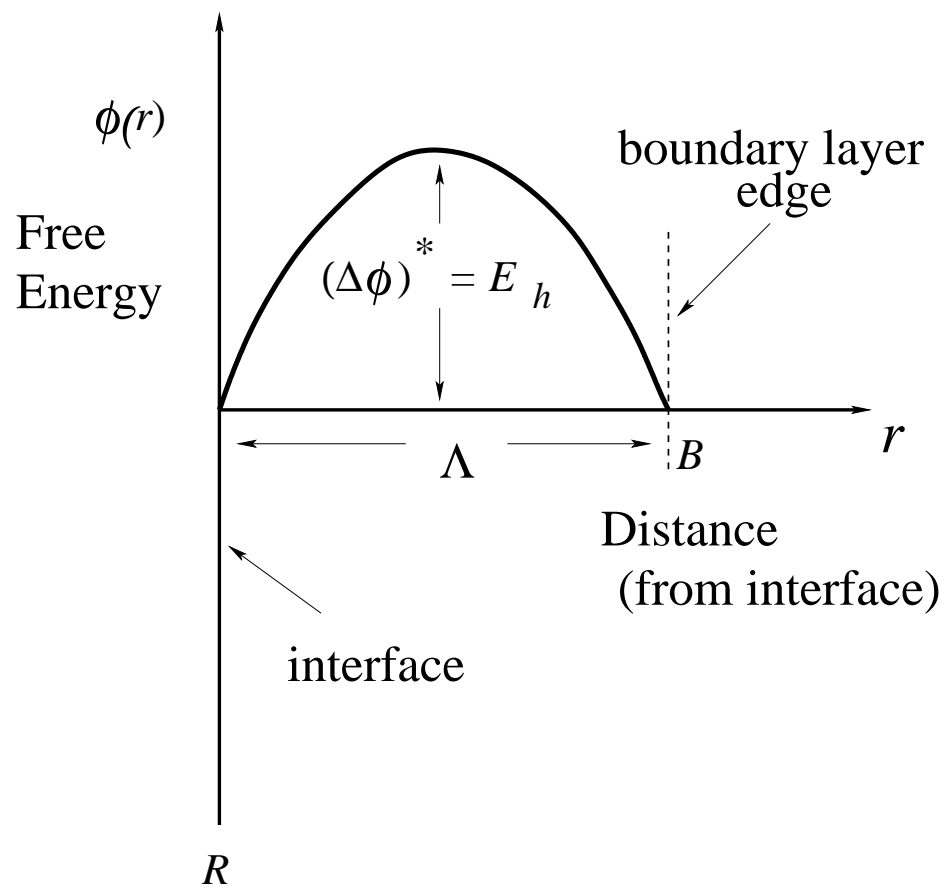


FIG. 4: Kundagrami *et al.*, *JCP*

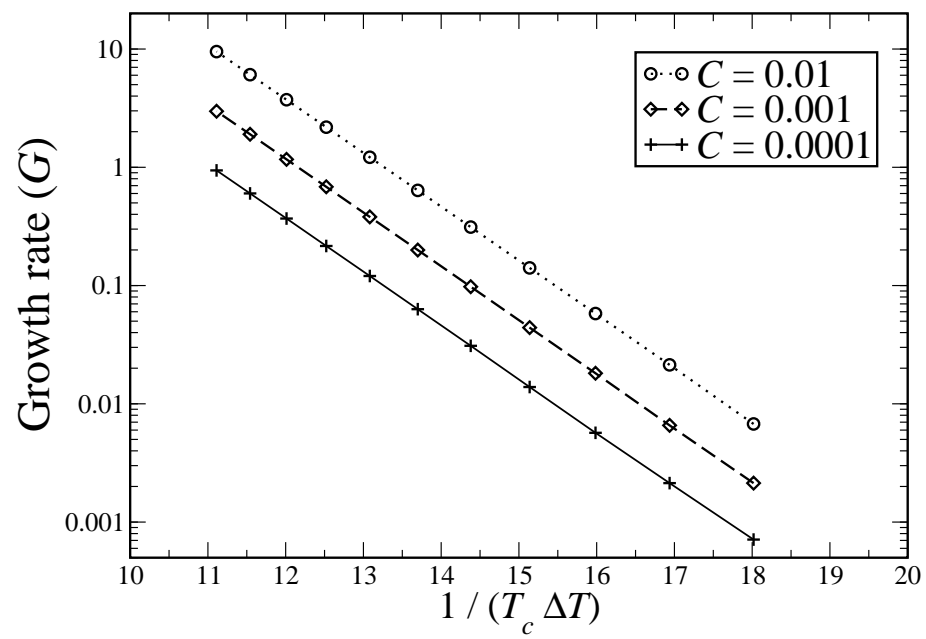


FIG. 5: Kundagrami *et al.*, *JCP*

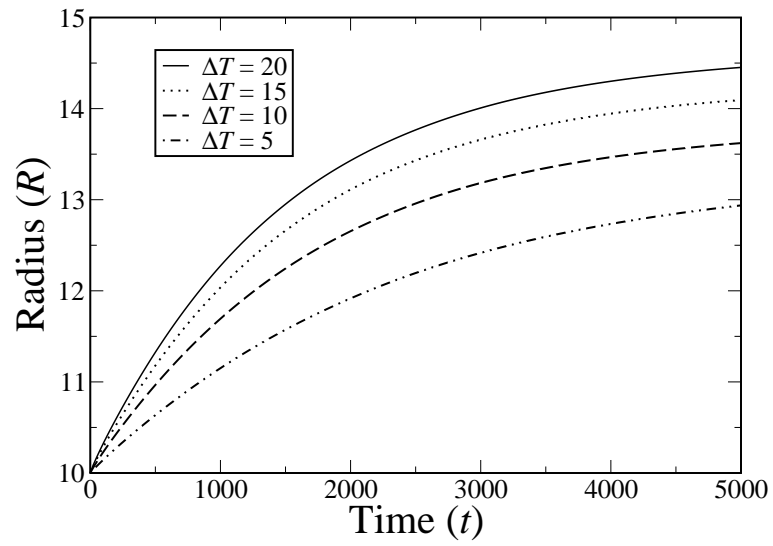
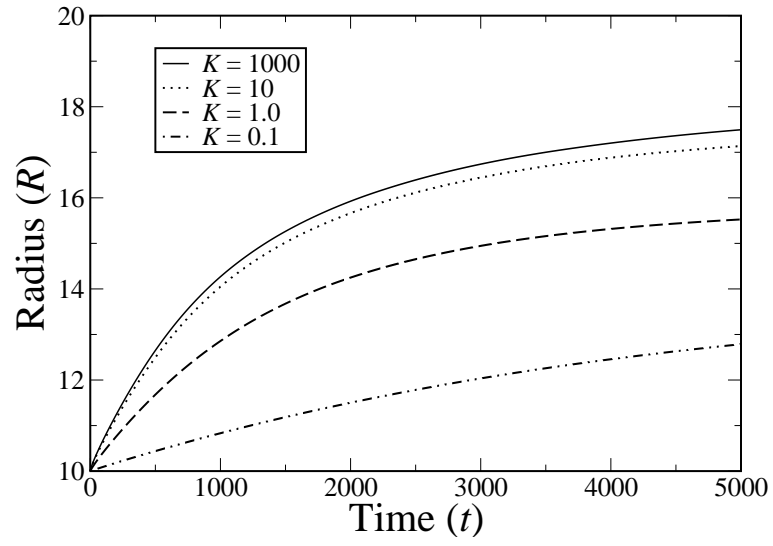
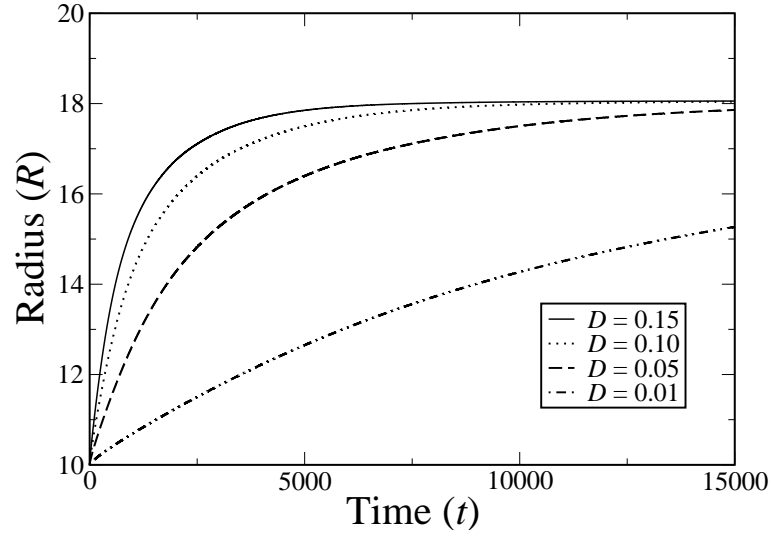


FIG. 6: Kundagrami *et al.*, *JCP*

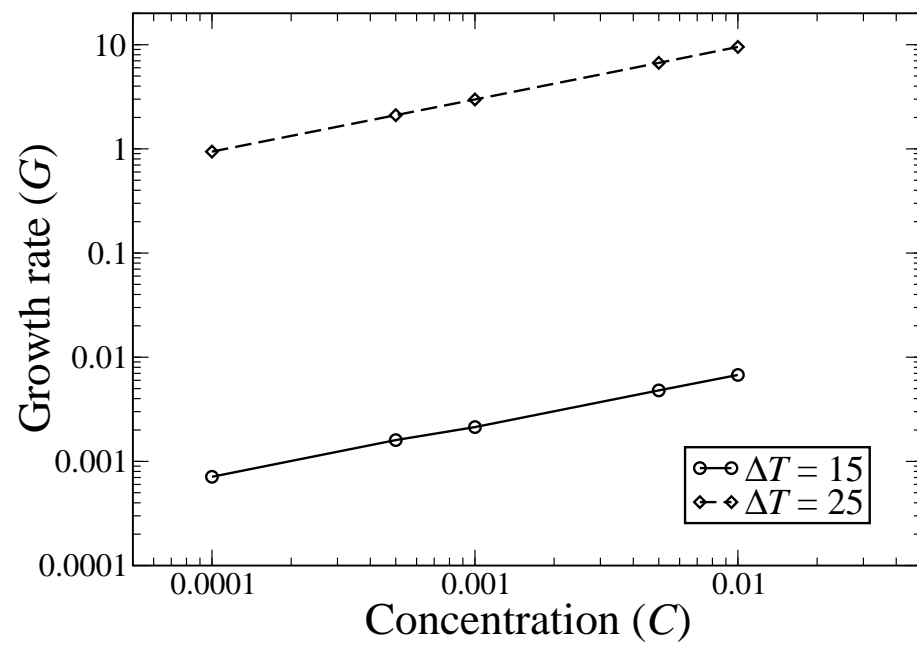


FIG. 7: Kundagrami *et al.*, *JCP*

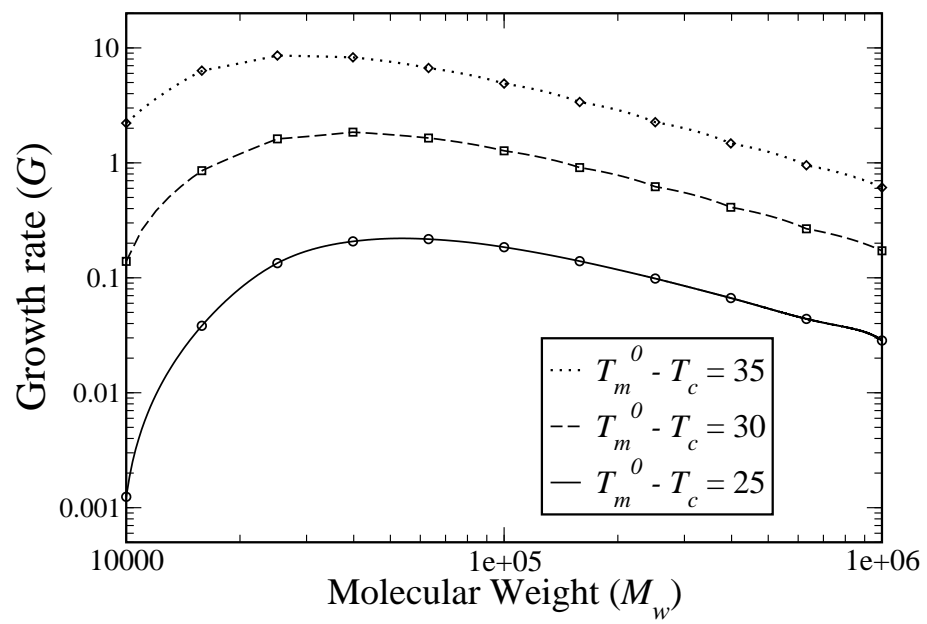


FIG. 8: Kundagrami *et al.*, *JCP*